Draft version December 2, 2024
Typeset using LaTeX **twocolumn** style in AASTeX63

Searching for TTVs in young transiting systems

Ana Isabel Lopez Murillo,[1,*] Andrew W. Mann,[1] Madyson G. Barber,[1,†] Andrew Vanderburg,[2] Pa Chia Thao,[1,‡] and Andrew W. Boyle[1]

[1] *Department of Physics and Astronomy, The University of North Carolina at Chapel Hill, Chapel Hill, NC 27599, USA*
[2] *Department of Physics and Kavli Institute for Astrophysics and Space Research, Massachusetts Institute of Technology, Cambridge, MA 02139, USA*

ABSTRACT

The discovery of young (<800 Myr) transiting planets has provided a new avenue to explore how planets form and evolve over their lifetimes. Mass measurements for these planets would be invaluable, but radial velocity surveys of young systems are often overwhelmed by stellar activity. Transiting timing variations (TTVs) offer an alternative route to masses that are less impacted by signals from the host star. Here we search for TTVs in a sample of 40 young systems hosting 59 transiting planets using data from *Kepler* *K*2 and *TESS*. We recover previously reported TTVs in AU Mic, TOI-2076, and TOI-1227, and identify new TTVs in XXX systems, including the 17 Myr planet HIP 67522 b. We show that these TTVs are not an artifact of spots or other challenges specific to young stars. BB of the systems (name them) have only a single detected transit, motivating a search for additional planets. None of the TTVs detected in multi-transiting systems are sufficient for a measurement of the planets' masses. However, these discoveries should drive more transit observations required to fully characterize the signal and eventually measure the masses.

1. INTRODUCTION

A long-standing question in exoplanet research is to understand how planets evolve over their lifetimes. The simplest observational path to answer this question is to compare the properties of planets as a function of age. However, the majority of discovered planetary systems are either old (>1 Gyr) or have unknown ages. Fortunately, the *K*2 and *TESS* missions surveying nearby young clusters and associations has led to the discovery of > 40 young (10-700 Myr), transiting planets (Barber et al. 2022; Newton et al. 2022; Mann et al. 2020).

Theoretical models predict that young ($\ll$ 1 Gyr) planets will be larger than their older counterparts due to the retained heat from their formation that causes their atmosphere to expand (Lopez et al. 2012). However, there are a range of physical drivers, and it remains unclear which is the most important. Low-mass, H/He-rich planets can shrink by a factor of $\simeq$2 in radius between 50 Myr and 500 Myr due to thermal contraction (Lopez & Fortney 2014). Young planets may also appear larger because of the presence of photochemical hazes that render their atmospheres opaque (Gao & Zhang 2020). Alternatively, the low surface gravity and high irradiation of most young planets make them vulnerable to atmospheric mass-loss through photo-evaporation (Murray-Clay et al. 2009), driving the planets to smaller radii as material of low mean molecular weight is lost. All these processes operates on a different duration and studying young planets will provide a timescale for changes.

Masses for a sample of the young planets are essential to break these degeneracies and provide a more quantitative test of planetary evolution models. Without a mass, a young planet may appear to have a similar radius as an older planet, but still be significantly inflated if it is less massive. Without accurate mass estimates, it is difficult to interpret the detection of features in transmission spectra, as there are strong degeneracies between surface gravity and composition (Batalha et al. 2017). Further, masses are essential to perform a fair comparison between old and young planetary systems given the complex relation between period, radius, and migration history.

Radial velocity work in young systems has proven to be challenging. The mass detection of the 30 Myr V1298 Tau e from Suárez Mascareño et al. (2021) finds an orbital period that is 4σ discrepant with the follow-

Corresponding author: Ana Isabel Lopez Murillo
* UNC Chancellor's Science Scholar
† NSF Graduate Research Fellow
‡ NSF Graduate Research Fellow
Jack Kent Cooke Foundation Graduate Scholar

up transit data in Feinstein et al. (2022), and in conflict with more extensive RV data (Sikora et al. 2023; Blunt et al. 2023). Zakhozhay et al. (2022) find a mass of $8\pm1 M_J$ for the 15 Myr Jupiter-radius planet HD 114082 b, but even cold-star models predict a mass below $1 M_J$ at this age (Spiegel & Burrows 2012), and the the report of a second *larger* planet in the system (ExoFOP 2019) likely invalidates the analysis. A number of other systems have been the subject of extensive monitoring campaigns and only yielded upper limits on mass (e.g., Benatti et al. 2021; Damasso et al. 2023). Similarly concerning is that youngest planets discovered through radial velocities are not consistently recovered (e.g., Donati et al. 2020; Damasso et al. 2020).

It is possible to estimate the mass of a planet through its transmission spectrum, by taking advantage of the relation between the scale height and the planet's surface gravity (de Wit & Seager 2013). Applying this method to small planets is challenging due to degeneracies between metallicity, cloud cover, and surface gravity (Batalha et al. 2017). The method has worked, however, on young gas giants (Thao et al. 2024b). Such systems tend to have lower surface gravity than their older counterparts, making it easier to break the degeneracies. This method may still fail for the smallest planets, and measuring masses for a large sample of young planets would require an unrealistic amount of *JWST* data.

An alternative route for precision masses of young planets is Transit Timing Variations (TTVs) – changes in the planet's transit time due to the gravitational influence of another object. TTVs have provided masses for small planets (Jontof-Hutter et al. 2015) and a limited set of young stars (e.g. Masuda 2014). Importantly, young planets are found near mean-motion resonances (MMR) at a much higher rate than for older planets (e.g., 86±13% of multis <100 Myr; Dai et al. 2024). Since TTV signals are much larger for planets near MMR, we expect a similarly high fraction of young multi-transiting systems to show TTVs.

Often a detected TTV is insufficient to constrain the full system parameters. It is not possible to break degeneracies between eccentricity and mass in many systems, for example (Becker et al. 2015). However, such TTVs may still be useful for setting limits on eccentricity and mass, detect additional planets in the system, and motivate future ground-based studies to fully map out the TTV signal.

Here we search for signs of TTVs in young transiting planets with *Kepler K2* and/or *TESS* data. In Section 2 we list the young systems of interest. We describe the light curve data in Section 4. We then detail our method for fitting individual transits and searching for TTVs in Section 5. In Section 6 we overview which systems show significant TTVs and the role of spots on the TTV signal. We conclude in Section 7 with a discussion of which TTVs show the best promise for mass detections in the immediate future.

2. TARGET SELECTION

We initially selected all transiting planets with ages <800 Myr and age uncertainties < 100 Myr. The former cut is roughly Hyades age or younger, where stellar activity can make radial velocities more challenging (Cochran et al. 2002; Paulson et al. 2004; Brems et al. 2019). The latter is meant to remove targets with highly uncertain ages, many of which are likely to be >1 Gyr due to a strong bias in favor of older systems in the transiting planet sample. We drew this list from a mix of the NASA exoplanet archive (Foreman-Mackey et al. 2021) and a search of recent literature (e.g., Newton et al. 2022).

The sample was finalized in September, 2024. Planets discovered after this date were not included. The exception was IRAS 04125+2902 b, which already included an (identical) TTV analysis to that performed here.

From this list we removed four systems. HD 114082 (Zakhozhay et al. 2022) and HD 283869 (Vanderburg et al. 2018) are both single-transiting systems, for which TTV detections will not be possible. Kepler-411 has a reported age of 200 Myr (Sun et al. 2019), but the host star shows no detectable lithium (Berger et al. 2018) and the 10.5 day rotation period and color puts it in the 'stalling' regime (Curtis et al. 2019). In combination, this suggests an age of at least 600 Myr. TOI-560 has the same problem; no lithium and a rotation period consistent with 0.1–1.4 Gyr. While it is possible these meet our age criteria, they do not meet our age uncertainty criteria, so we opted to remove them.

This left 62 planets orbiting 42 stars. The majority have robust ages derived from membership to a young association, but many have ages derived from a combination of gyrochronology and similar indicators of age (e.g., lithium). We provide a full list in Table 3.

3. INPUT LIGHT CURVES

Table 1. Overview of Input Light Curves

System	planet	TESS sectors	Other input data	Total Time Span	$N_{\rm transits}$	Significance	Parameters
			(days)	(years)		$\chi^2/d.o.f$	
AU Mic	b	1, 27	-	2	5	4.23	87
AU Mic	c	1, 27	-	2	3	4.76	87
DS Tuc A	b	1, 27, 28, 67, 68	-	5.5	15	3.28	63
HD 110082	b	12, 13, 27, 65, 66, 67	-	4.4	16	0.90	83
HD 63433	b	20, 44, 45, 46, 47, 72	-	2.3	17	1.01	67; 15
	c	20, 44, 45, 46, 47, 72	-	2.3	8	6.44	67; 15
	d	20, 44, 45, 46, 47, 72	-	2.3	29	2.30	67; 15
HD 178085	b	27, 66, 67	-	3.3	6	1.09	91; 55
HIP 67522	b	11, 38, 64	-	4	10	0.32	4
	c	11, 38, 64	-	4	5	0.63	4
IRAS04125+2902	b	19, 43, 44, 59, 70, 71	-	-	16	0.80	
K2 100	b	44, 45, 46, 72	K2 Campaign 5, 18	4.34	128	0.94	5; 73
K2 101	b	-	K2 Campaign 5, 16, 18	3.14	13	0.62	16; 51
K2 102	b	-	K2 Campaign 5, 16, 18	3.15	20	0.11	51
K2 103	b	-	K2 Campaign 5, 16, 18	3.3	10	1.50	16; 27
							51
K2 104	b	-	K2 Campaign 5, 16, 18	3.3	100	0.3	16; 27
							51
K2 136	b	-	K2 Campaign 13	0.25	8	4.59	57
	c	-	K2 Campaign 13	0.25	4	5.09	57; 43
	d	-	K2 Campaign 13	0.25	3	1.54	57; 47
K2 233	b	-	K2 Campaign 15	0.25	35	1.08	46
	c	-	K2 Campaign 15	0.25	11	1.12	46
	d	-	K2 Campaign 15	0.25	3	2.91	46
K2 25	b	44,70,71	K2 Campaign 15	2.95	37	0.26	74
K2 264	b	-	K2 Campaign 16	0.25	13	0.95	48
	c	-	K2 Campaign 16	0.25	4	6.01	48
K2 284	b	-	K2 Campaign 13	0.25	12	1.22	24
Kepler 1627	b	-	Kepler Q1-15	3.01	127	0.55	60
Kepler 1643	b	-	Kepler Q1-17	4.11	252	0.38	13
Kepler 51	b	-	Kepler Q1-17	7	32	21.5	56; 45
Kepler 51	c	-	Kepler Q12-17	1.36	6	4.69	56; 45

Table 1 *continued*

Table 1 *(continued)*

System	planet	TESS sectors	Other input data	Total Time Span	$N_{\rm transits}$	Significance	Parameters
			(days)	(years)		$\chi^2/d.o.f$	
Kepler 51	d	-	Kepler Q1-17	7	10	52.07	56; 45
Kepler 63	b	14,15,40,41,53,54,55,74,75,80,81,82	Kepler Q2-17	9.2	164	1.06	69
Kepler 970	b	-	Kepler Q1-17	4.11	80	0.77	3
Kepler 1928	b	-	Kepler Q1-17	4.11	72	0.13	3
KOI 7913 A	b	-	Kepler Q1-18	4.11	55	0.52	13
Qatar 3	b	57	-	0.15	9	0.34	1; 43
Qatar 4	b	57	-	0.15	12	0.49	1; 43
Qatar 5	b	14,17,57	-	3.15	15	1.05	1; 43
TOI 1227	b	11, 12, 38, 64, 65	-	4.11	5	5.71	54
TOI 1807	b	22,23,49,76	-	3.56	140	1.08	67; 62
TOI 2048	b	16,23,24,50,51,77,78	-	3	9	0.53	65
TOI 251	b	1,2,29,69	-	5.5	14	0.36	90
TOI 451	b	4,5,31	-	2.2	37	0.60	64
	c	4,5,31	-	2.2	8	0.87	64
	d	4,5,31	-	2.2	5	0.84	64
TOI 942	b	5, 32	-	2	11	0.52	
TOI 942	c	5, 32	-	2	5	0.86	
TOI 1860	b	14,15,16,21,22,23,41,48,49,50,75	-	4.95	307	0.46	36
TOI 837	b	10,11,37,38,63,64	-	4.5	19	1.17	6; 12
TOI 1097	b	38, 39	-	0.16	6	1.92	88
TOI 1097	c	38,39	-	0.16	-	-	88
TOI 2076	b	16,23,50,77	-	-	9	3.17	67; 43
TOI 2076	c	16,23,50,77	-	-	3	1.01	67; 38
TOI 2076	d	16,23,50,77	-	-	3	7.97	67; 38
V1298 Tau	b	42,43,44	K2 Campaign 4	1	5	5.18	23; 29
V1298 Tau	c	42,43,44	K2 Campaign 4	1	15	2.26	23; 29
V1298 Tau	d	42,43,44	K2 Campaign 4	1	9	10.26	23; 29
V1298 Tau	e	42,43,44	K2 Campaign 4	1	3	13.15	23; 29
							31
TOI 1224	b	1-13, 27, 28, 39, 66-68	-	-	-	-	
	c	1-13, 27, 28, 39, 66-68	-	-	-	-	
TOI 1227	b	1-13, 27, 28, 39, 66-68	-	5	50	-	
	c	1-13, 27, 28, 39, 66-68	-	5	50	-	

4. LIGHT CURVES

We used light curves from *Kepler*, *K*2 and *TESS*, where possible. While nearly all targets have *TESS* data, many planets detected in *K*2 or *Kepler* data orbit stars that are too faint or land in fields too crowded to make full use of the *TESS* data. Further, for our TTV analysis, it is important that each individual transit be detectable to extract a usable transit time. For some smaller planets, the signal is only significant over the full curve, particularly in the *TESS* data. We list what datasets were included for each planet in Table 3.

4.1. *TESS*

For young active stars, the default *TESS* data processing can fail due to complications separating instrumental and stellar signals (e.g., Taaki et al. 2024). We follow the systematics correction to the simple aperture photometry (SAP) from the SPOC pipeline (Jenkins et al. 2016) outlined in Vanderburg et al. (2019). This method has dramatically improved the noise properties of the light curves for young stars (e.g. Barber & Mann 2023; Thao et al. 2024a).

We confirm the superiority of the modified pipeline by analyzing one system (HIP 67522 b and c) with both PDCSAP (Pre-search Data Conditioning SAP) and the Vanderburg et al. (2019) method. While the results were broadly consistent, the fit was better (better reduced χ^2) using the Vanderburg et al. (2019) light curves. The analysis using PDCSAP curves also yielded much smaller uncertainties on the transit times, suggesting timing variations even over just 2-3 consecutive transits.

In total, YY stars have *TESS* data sufficient for our analysis.

4.2. *Kepler*

For XX systems with *Kepler* data, we used the Pre-search Data Conditioning Simple Aperture Photometry (PDCSAP; Smith et al. 2012; Stumpe et al. 2014) light curve produced by SPOC and available through Mikulski Archive for Space Telescopes (MAST) [1].

In order to ensure data reliability, we only considered data points with `DQUALITY=0`, indicating that no flags were raised by the SPOC pipeline.

4.3. *K2*

The *K*2 mission operated short one reaction wheel, causing the telescope to shift. During the drift and subsequent thruster fire a stellar image moves over the detector. Combined with variations in the pixel sensitivity this generates changes in estimated flux from a given star as a function of centroid position. To correct for this, we used the light curves from the K2SFF pipeline (Vanderburg & Johnson 2014). Curves from K2SFF have been used widely for the analysis of young systems (Mann et al. 2017,?; Rizzuto et al. 2017)

Stellar variability in young stars can operate on timescales comparable to the telescope drift, which can sometimes cause the extraction to fail. Some analyses have therefore used a simultaneous fit of the variability and the instrumental systematics (e.g., Mann et al. 2018; Thao et al. 2020). Tests with this seemed to have no impact on the transit times for a sample of systems considered here. So, we opted to use the K2SFF light curves without additional corrections.

In total, ZZ systems had usable *K*2 data.

5. METHODS

5.1. *Measuring Individual Transit Times*

A summary of our process is:

1. For each planet, we download all available light curve data (see subsections above).
2. We take initial planet parameters from the NASA Exoplanet Archive as noted in Table 3. In some cases, we retrieve parameters directly from the paper.
3. We fit each transit using a `BATMAN` model (Kreidberg 2015) and a Gaussian Process (GP) to handle stellar variability.
4. We inspect the fits and the TTV residual (O-C). Some fits are removed or adjusted and redone based on this assessment.
5. We characterize the significance of the TTV using a flat-line fit and computing the reduced χ^2 ($\chi^2_n\nu$).

For each transit fit (step 3), we locked all parameters to the literature value except the transit midpoint (T_0) and three GP parameters. For the GP, we use a simple harmonic oscillator (SHO) as implemented in `Celerite` (Foreman-Mackey 2018). This includes three free parameters, the standard deviation of the process (σ), the underdamped period of the oscillator (ρ), and the quality factor (Q). Tests using simpler polynomials yielded poor fits to the data. Other quasi-periodic kernels worked similarly well, although we preferred the SHO kernel because of a long history of success on young stellar systems (e.g., Thao et al. 2023; Wood et al. 2023; Barber et al. 2024).

[1] https://mast.stsci.edu/portal/Mashup/Clients/Mast/Portal.html

Table 2. Time of Transit and O-C Posteriors for TOI-1224c

Transit Number	Prior[a]	Posterior	O-C (min)
T_0	$\mathcal{U}(2458329.8653, 0.03)$	$2458329.8680^{+0.0015}_{-0.0015}$	3.92 ± 2.21
T_1	$\mathcal{U}(2458347.8107, 0.03)$	$2458347.8111^{+0.0024}_{-0.0027}$	0.63 ± 4.76
T_{19}	$\mathcal{U}(2458670.8287, 0.03)$	$2458670.8163^{+0.0022}_{-0.0032}$	-17.78 ± 4.43
T_{40}	$\mathcal{U}(2459047.6831, 0.03)$	$2459047.6740^{+0.0020}_{-0.0020}$	-13.04 ± 6.11
T_{41}	$\mathcal{U}(2459065.6285, 0.03)$	$2459065.6224^{+0.0043}_{0.0057}$	-8.77 ± 7.98
T_{42}	$\mathcal{U}(2459083.5740, 0.03)$	$2459083.5632^{+0.0025}_{0.0028}$	-15.48 ± 4.04
T_{58}	$\mathcal{U}(2459370.7010, 0.03)$	$2459370.6883^{+0.0019}_{0.0019}$	-18.41 ± 3.37
T_{59}	$\mathcal{U}(2459388.6465, 0.03)$	$2459388.6376^{+0.0034}_{0.0041}$	-12.84 ± 5.64
T_{99}	$\mathcal{U}(2460106.4642, 0.03)$	$2460106.4638^{+0.0033}_{0.0031}$	-0.61 ± 7.88
T_{101}	$\mathcal{U}(2460142.3551, 0.03)$	$2460142.3535^{+0.0025}_{0.0023}$	-2.30 ± 4.58
T_{102}	$\mathcal{U}(2460160.3006, 0.03)$	$2460160.2959^{+0.0017}_{0.0018}$	-6.75 ± 2.67
T_{103}	$\mathcal{U}(2460178.2460, 0.03)$	$2460178.2391^{+0.9923}_{0.0020}$	-10.04 ± 3.39

[a] $\mathcal{U}(a, b)$ indicates a uniform distribution between a and b.

The transit fits were done using a Monte Carlo Markov Chain framework with `emcee` (Foreman-Mackey et al. 2013). All parameters evolved under uniform priors. Every transit runs for 10,000 steps with 30 walkers. This was sufficient for convergence in most cases (Goodman & Weare 2010). If the solution had not yet converged, the run was extended for an additional 10,000 steps.

We show an example transit fit in Figure 1. This star has a short rotation period (1.39 days; Heitzmann et al. 2021) creating significant variability on timescales comparable to that of the planets transit duration. However, the GP correctly models the stellar signal and yields a residual consistent with white noise.

We show an example fit posterior in Figure 2. The resulting transit time posteriors were almost universally Gaussian. Those deviating from a Gaussian were those with Gaussian cores with wider tails or slight asymmetry. For simplicity, we opted to convert these to one-dimensional uncertainties when computing the TTV signal.

Using the literature reported period and T_0, we computed the difference between the expected and measured transit times (the O-C). Some systems showed linear trend or systematic offset from zero, indicating an erroneous period or T_0. In these cases we fit for a new period and/or T_0 from our data and, when needed, reanalyzed the light curves.

We then compared the resulting O-C points to a flat-line model and compute a reduced χ^2 (χ^2_ν). The resulting χ^2_ν are reported in Table 3 for each planet and are the main metric we used for characterizing the likelihood of a TTV.

6. RESULTS

We show the histogram of χ^2_ν values in Figure **??**.

Over-fitting was observed for several systems with positive known TTVs, including the system HIP 67522. Due to large uncertainties in *K2* and *Kepler* data, many planets with these data were found to have a χ^2_ν of $<$ 1. Similar observations of over-fitting in other systems prompted us to shift our χ^2_ν metric for significance of a TTV from 1 to 1.05.

HIP 67522 b also showed slightly more significant TTVs using the PDCSAP data rather than the SPOC pipeline. The O-C results from our analysis using the SPOC pipeline were similar but with larger uncertainties, driving the χ^2_ν down.

We show an example fit of a transit in Figure 1. HIP 67522 b has strong stellar variability due to its young age, prompting us to inspect fits by eye to measure whether the GP was handling variability sufficiently. Fig 3 shows the first transit of TOI-837 b, with stellar variability removed from the GP. Coupled with other fits, we concluded that the GP was sufficiently handling stellar variability to reveal noticeable offsets in transit time.

We show an example O-C plot in Figure 4. We recovered significant TTVs in known systems, including AU Mic, V1298 Tau, and TOI 1224. We report new TTVs in the systems HIP 67522, TOI 837, and TOI 1097. These systems exhibit a χ^2_ν of greater than 1.06, implying significant variations caused by gravitational interactions with another planetary body in the system. Of these, both HIP 67522 and TOI 1097 are two-planetary systems in mean motion resonance. Due to the near integer ratios of their planetary periods, TTVs for these systems are easier to quantify and visualize using a sine-wave function, and show up with higher significance in

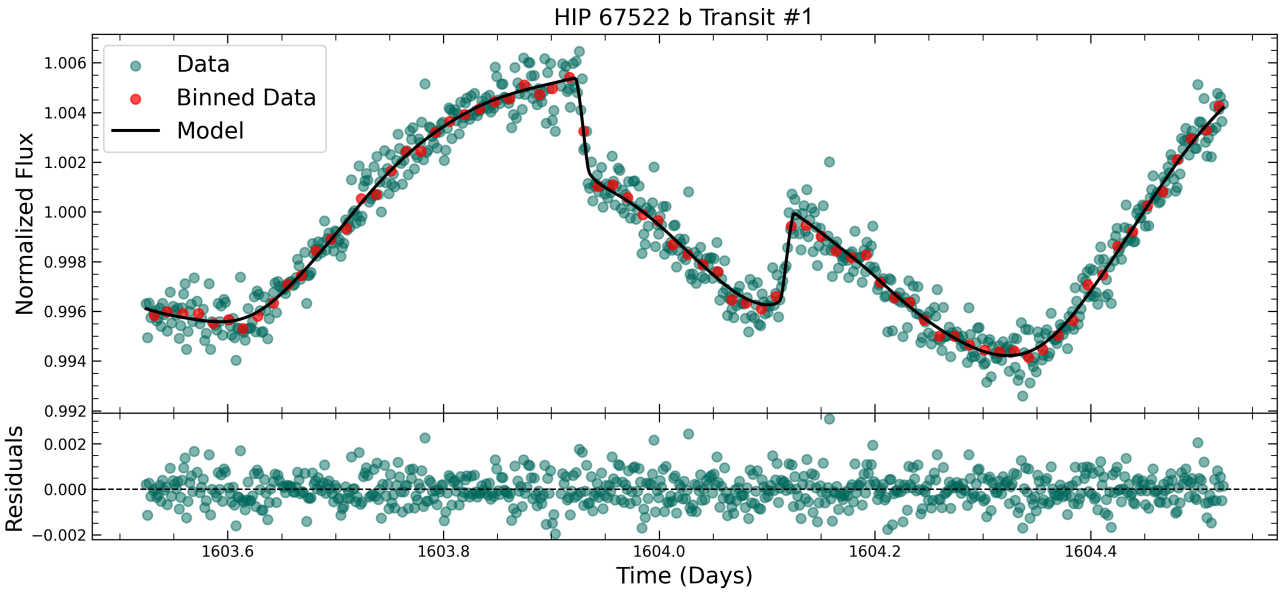

Figure 1. The first transit of HIP 67522 b (green points) and the best-fit model (black). For clarity, we also show the data binned to 20 minutes (red points). The bottom panel shows the best-fit residuals, which are generally consistent with white noise and suggest the GP is handling the strong stellar variability well.

χ^2_ν evaluations Masuda (2014). TOI 837 is a reported single-planetary system, and TTV significance found of 1.17 could be used to motivate future follow-up for detection of a second planet in the system and mass follow-up.

Due to the large uncertainties of the data of many systems, follow-up observations of many systems would be helpful to constrain TTVs.

6.1. *Can spots explain some TTVs?*

Young stars often exhibit fast rotation (Cody et al. 2017) and significant starspot coverage (Morris 2020; Barber & Mann 2023). If the planet crosses a spot, especially near ingress or egress, it can introduce a TTV due to changes in the shape of the transit. However, the resulting TTV will correlate to the flux derivative (Mazeh et al. 2015), which is detectable in the same dataset. In this way, one can separate TTVs from dynamical interactions versus those from stellar activity (Holczer et al. 2015).

7. CONCLUSIONS AND DISCUSSION

ACKNOWLEDGMENTS

AWM was supported by grants from the NSF CAREER program (AST-2143763) and NASA's exoplanet research program (XRP 80NSSC21K0393). MGB was supported by NSF Graduate Research Fellowship (DGE-add numbers).

This paper includes data collected by the TESS mission. Funding for the TESS mission is provided by the NASA's Science Mission Directorate.

Software:

Facilities:

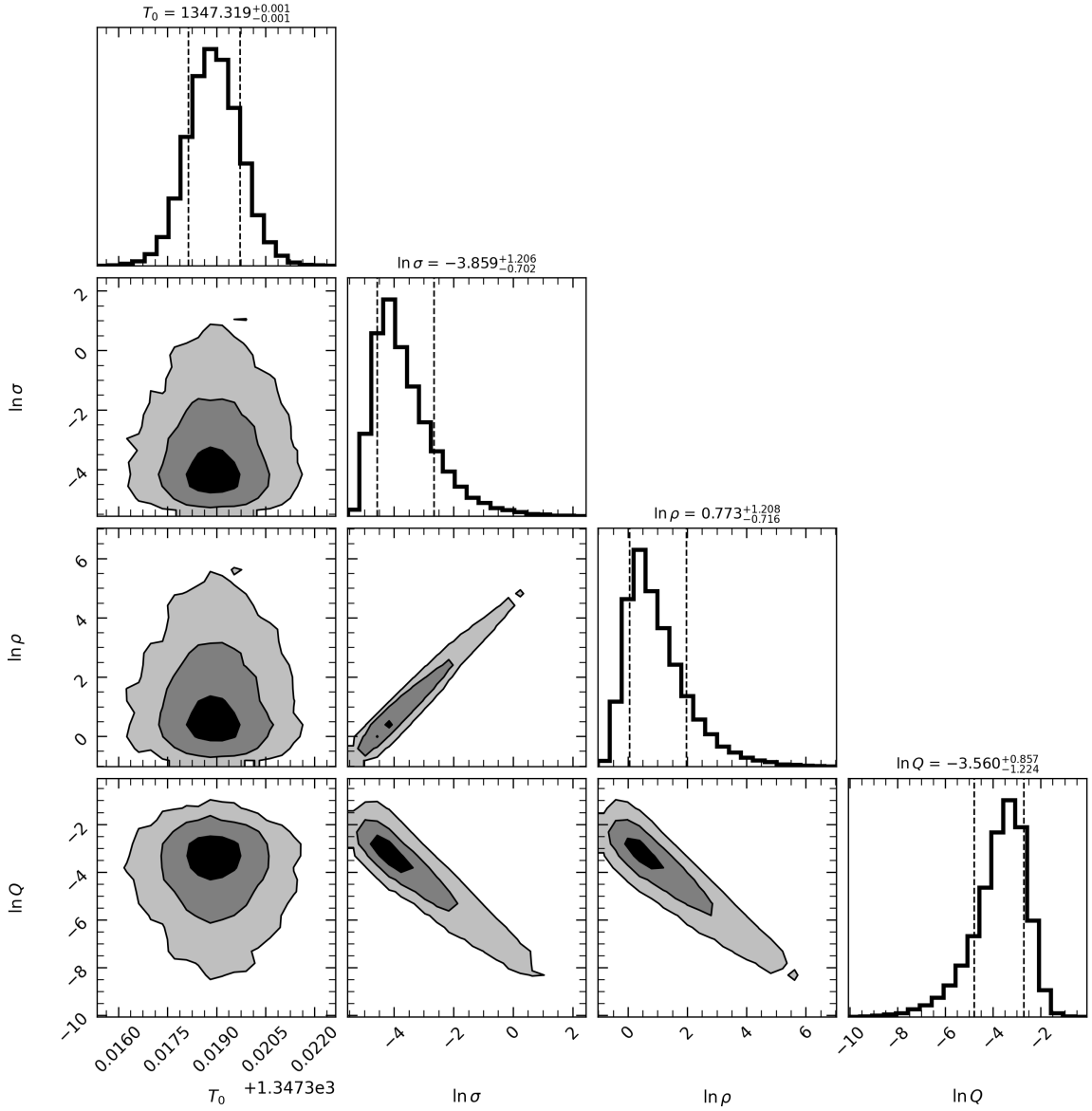

Figure 2. Corner plot for the second transit of AU Mic b.

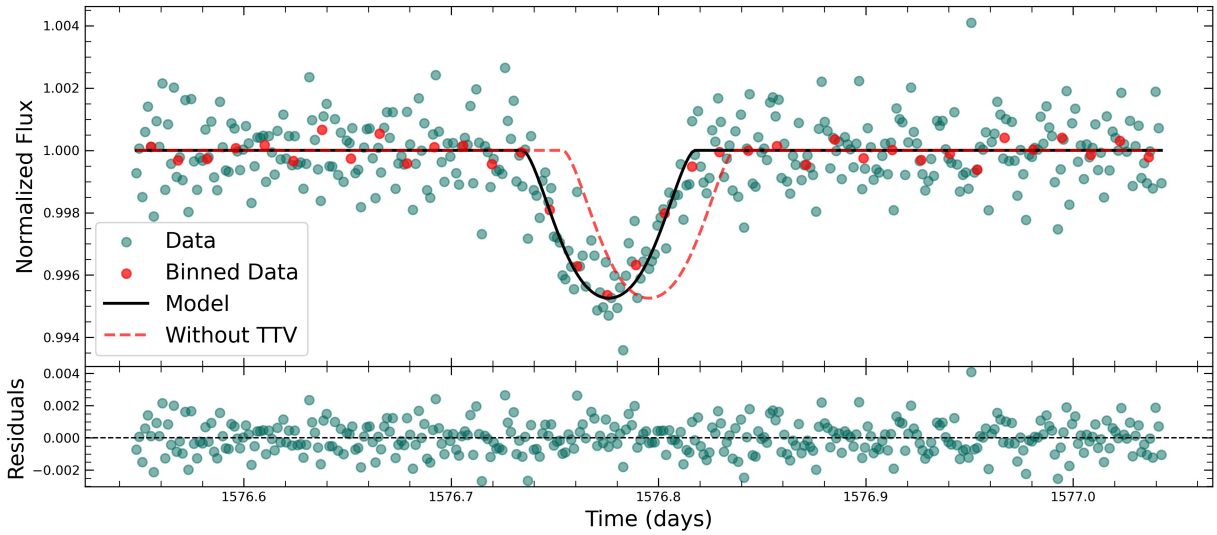

Figure 3. First transit of TOI-837 b, with a O-C value of -27.97 minutes. Stellar variability has been removed with the GP model, showing the detrended fit. Red dots represent data binned to 20 minutes.

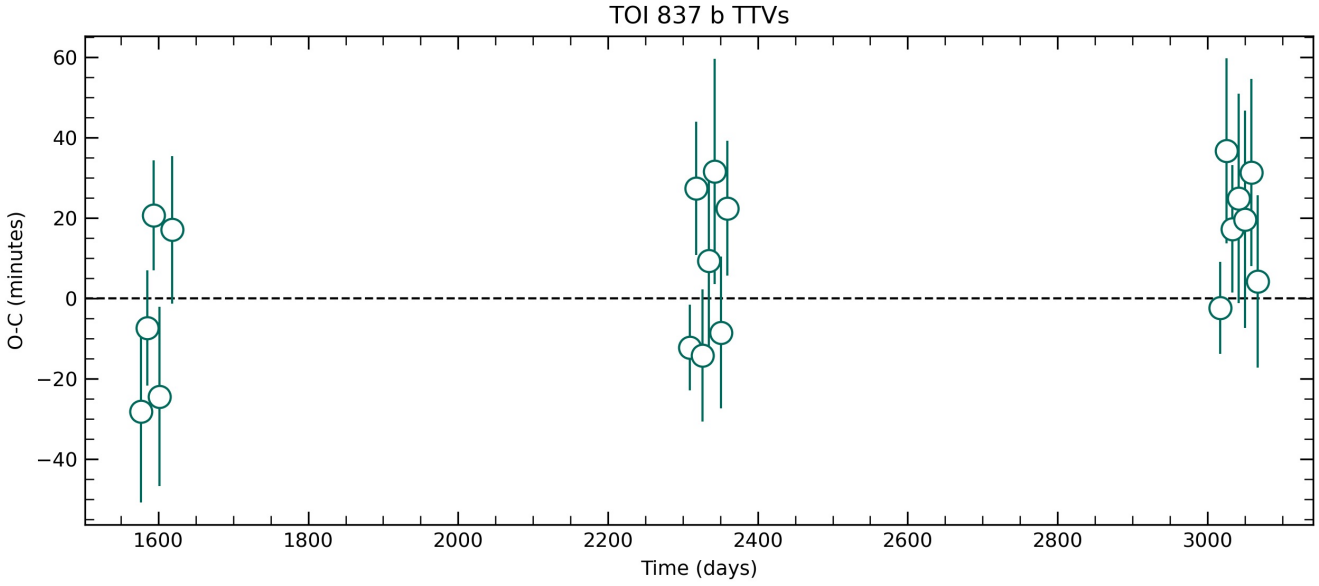

Figure 4. Observed - Calculated (O-C) plot for TOI-837 b, with a χ^2_ν of 1.17.

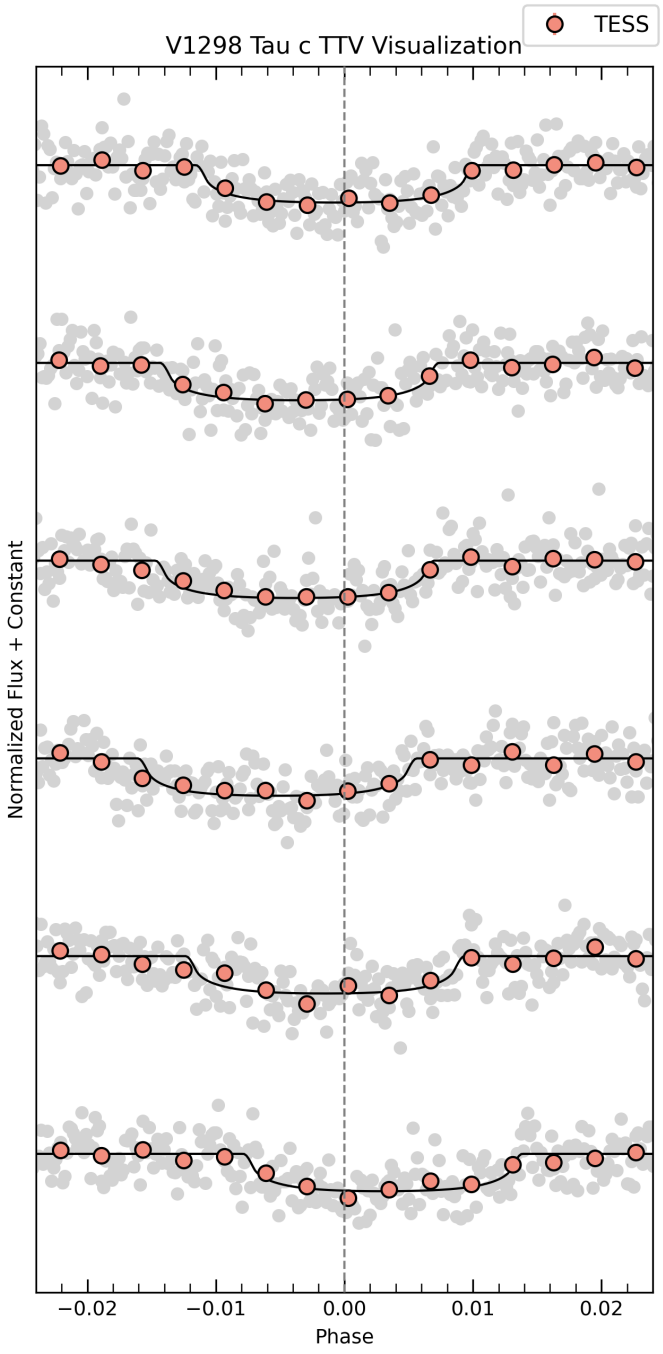

Figure 5. Phase-folded light curve of V1298 Tau c transits taken with *TESS* (orange). Our best-fit model is overlaid in a black line. Circular dots represent data binned into 4.5 minute intervals.

REFERENCES

Alsubai, K., Mislis, D., Tsvetanov, Z. I., et al. 2017, AJ, 153, 200

Barber, M. G., & Mann, A. W. 2023, arXiv e-prints, arXiv:2302.09084

Barber, M. G., Mann, A. W., Bush, J. L., et al. 2022, arXiv e-prints, arXiv:2206.08383

Barber, M. G., Thao, P. C., Mann, A. W., et al. 2024, arXiv e-prints, arXiv:2407.04763

Barragán, O., Aigrain, S., Kubyshkina, D., et al. 2019, MNRAS, 490, 698

Barragán, O., Yu, H., Freckelton, A. V., et al. 2024, MNRAS, 531, 4275

Batalha, N. E., Kempton, E. M. R., & Mbarek, R. 2017, ApJL, 836, L5

Becker, J. C., Vanderburg, A., Adams, F. C., Rappaport, S. A., & Schwengeler, H. M. 2015, ApJL, 812, L18

Benatti, S., Damasso, M., Borsa, F., et al. 2021, A&A, 650, A66

Berger, T. A., Huber, D., Gaidos, E., & van Saders, J. L. 2018, ApJ, 866, 99

Blunt, S., Carvalho, A., David, T. J., et al. 2023, AJ, 166, 62

Bouma, L. G., Hartman, J. D., Brahm, R., et al. 2020, AJ, 160, 239

Bouma, L. G., Kerr, R., Curtis, J. L., et al. 2022, AJ, 164, 215

Brems, S. S., Kürster, M., Trifonov, T., Reffert, S., & Quirrenbach, A. 2019, A&A, 632, A37

Capistrant, B. K., Soares-Furtado, M., Vanderburg, A., et al. 2024, AJ, 167, 54

Castro-González, A., Díez Alonso, E., Menéndez Blanco, J., et al. 2022, MNRAS, 509, 1075

Cochran, W. D., Hatzes, A. P., & Paulson, D. B. 2002, AJ, 124, 565

Cody, A. M., Hillenbrand, L. A., David, T. J., et al. 2017, ApJ, 836, 41

Curtis, J. L., Agüeros, M. A., Douglas, S. T., & Meibom, S. 2019, ApJ, 879, 49

Dai, F., Goldberg, M., Batygin, K., et al. 2024, arXiv e-prints, arXiv:2406.06885

Damasso, M., Lanza, A. F., Benatti, S., et al. 2020, A&A, 642, A133

Damasso, M., Locci, D., Benatti, S., et al. 2023, A&A, 672, A126

David, T. J., Petigura, E. A., Luger, R., et al. 2019, AJ, 1910.04563

David, T. J., Mamajek, E. E., Vanderburg, A., et al. 2018, AJ, 156, 302

de Wit, J., & Seager, S. 2013, Science, 342, 1473

Donati, J. F., Bouvier, J., Alencar, S. H., et al. 2020, MNRAS, 491, 5660

Dressing, C. D., Vanderburg, A., Schlieder, J. E., et al. 2017, AJ, 154, 207

ExoFOP. 2019, Exoplanet Follow-up Observing Program - TESS, doi:10.26134/EXOFOP3

Feinstein, A. D., David, T. J., Montet, B. T., et al. 2021, AJ, 2111.08660

Feinstein, A. D., David, T. J., Montet, B. T., et al. 2022, ApJL, 925, L2

Finociety, B., Donati, J. F., Cristofari, P. I., et al. 2023, MNRAS, 526, 4627

Foreman-Mackey, D. 2018, Research Notes of the American Astronomical Society, 2, 31

Foreman-Mackey, D., Hogg, D. W., Lang, D., & Goodman, J. 2013, PASP, 125, 306

Foreman-Mackey, D., Savel, A., Luger, R., et al. 2021, exoplanet-dev/exoplanet v0.4.4, doi:10.5281/zenodo.1998447

Gao, P., & Zhang, X. 2020, ApJ, 890, 93

Giacalone, S., Dressing, C. D., Hedges, C., et al. 2022, AJ, 163, 99

Goodman, J., & Weare, J. 2010, Communications in Applied Mathematics and Computational Science, 5, 65

Hedges, C., Hughes, A., Zhou, G., et al. 2021, AJ, 162, 54

Heitzmann, A., Zhou, G., Quinn, S. N., et al. 2021, ApJL, 922, L1

Holczer, T., Shporer, A., Mazeh, T., et al. 2015, ApJ, 807, 170

Jenkins, J. M., Twicken, J. D., McCauliff, S., et al. 2016, in Society of Photo-Optical Instrumentation Engineers (SPIE) Conference Series, Vol. 9913, Proc. SPIE, 99133E

Jontof-Hutter, D., Rowe, J. F., Lissauer, J. J., Fabrycky, D. C., & Ford, E. B. 2015, Nature, 522, 321

Kokori, A., Tsiaras, A., Edwards, B., et al. 2023, ApJS, 265, 4

Kreidberg, L. 2015, PASP, 127, 1161

Libby-Roberts, J. E., Berta-Thompson, Z. K., Désert, J.-M., et al. 2020, AJ, 159, 57

Lillo-Box, J., Lopez, T. A., Santerne, A., et al. 2020, A&A, 640, A48

Livingston, J. H., Dai, F., Hirano, T., et al. 2018, AJ, 155, 115

—. 2019, MNRAS, 484, 8

Lopez, E. D., & Fortney, J. J. 2014, ApJ, 792, 1

Lopez, E. D., Fortney, J. J., & Miller, N. 2012, ApJ, 761, 59

Mann, A. W., Gaidos, E., Vanderburg, A., et al. 2017, AJ, 153, 64

Mann, A. W., Vanderburg, A., Rizzuto, A. C., et al. 2018, AJ, 155, 4
Mann, A. W., Johnson, M. C., Vanderburg, A., et al. 2020, AJ, 160, 179
Mann, A. W., Wood, M. L., Schmidt, S. P., et al. 2022, AJ, 163, 156
Mantovan, G., Montalto, M., Piotto, G., et al. 2022, MNRAS, 516, 4432
Masuda, K. 2014, ApJ, 783, 53
Mayo, A. W., Dressing, C. D., Vanderburg, A., et al. 2023, AJ, 165, 235
Mazeh, T., Holczer, T., & Shporer, A. 2015, ApJ, 800, 142
Morris, B. M. 2020, ApJ, 893, 67
Morton, T. D., Bryson, S. T., Coughlin, J. L., et al. 2016, ApJ, 822, 86
Murray-Clay, R. A., Chiang, E. I., & Murray, N. 2009, ApJ, 693, 23
Nardiello, D., Malavolta, L., Desidera, S., et al. 2022, A&A, 664, A163
Newton, E. R., Mann, A. W., Tofflemire, B. M., et al. 2019, ApJL, 880, L17
Newton, E. R., Mann, A. W., Kraus, A. L., et al. 2021, AJ, 161, 65
Newton, E. R., Rampalli, R., Kraus, A. L., et al. 2022, AJ, 164, 115
Paulson, D. B., Cochran, W. D., & Hatzes, A. P. 2004, AJ, 127, 3579
Polanski, A. S., Lubin, J., Beard, C., et al. 2024, ApJS, 272, 32
Rizzuto, A. C., Mann, A. W., Vanderburg, A., Kraus, A. L., & Covey, K. R. 2017, AJ, 154, 224
Sanchis-Ojeda, R., Winn, J. N., Marcy, G. W., et al. 2013, ApJ, 775, 54
Sikora, J., Rowe, J., Barat, S., et al. 2023, arXiv e-prints, arXiv:2304.00797
Smith, J. C., Stumpe, M. C., Van Cleve, J. E., et al. 2012, PASP, 124, 1000
Spiegel, D. S., & Burrows, A. 2012, ApJ, 745, 174
Stefansson, G., Li, Y., Mahadevan, S., et al. 2018, AJ, 156, 266
Stefansson, G., Mahadevan, S., Maney, M., et al. 2020, AJ, 160, 192
Stumpe, M. C., Smith, J. C., Catanzarite, J. H., et al. 2014, PASP, 126, 100
Suárez Mascareño, A., Damasso, M., Lodieu, N., et al. 2021, Nature Astronomy, 6, 232
Sun, L., Ioannidis, P., Gu, S., et al. 2019, A&A, 624, A15
Taaki, J. S., Kemball, A. J., & Kamalabadi, F. 2024, AJ, 167, 60
Thao, P. C., Mann, A. W., Johnson, M. C., et al. 2020, AJ, 159, 32
Thao, P. C., Mann, A. W., Gao, P., et al. 2023, AJ, 165, 23
Thao, P. C., Mann, A. W., Barber, M. G., et al. 2024a, AJ, 168, 41
Thao, P. C., Mann, A. W., Feinstein, A. D., et al. 2024b, arXiv e-prints, arXiv:2409.16355
Tofflemire, B. M., Rizzuto, A. C., Newton, E. R., et al. 2021, AJ, 161, 171
Vanderburg, A., & Johnson, J. A. 2014, PASP, 126, 948
Vanderburg, A., Mann, A. W., Rizzuto, A., et al. 2018, AJ, 156, 46
Vanderburg, A., Huang, C. X., Rodriguez, J. E., et al. 2019, ApJL, 881, L19
Wittrock, J. M., Plavchan, P. P., Cale, B. L., et al. 2023, AJ, 166, 232
Wood, M. L., Mann, A. W., Barber, M. G., et al. 2023, AJ, 165, 85
Zakhozhay, O. V., Launhardt, R., Trifonov, T., et al. 2022, A&A, 667, L14
Zhou, G., Quinn, S. N., Irwin, J., et al. 2021, AJ, 161, 2
Zhou, G., Wirth, C. P., Huang, C. X., et al. 2022, AJ, 163, 289